Chapter 15
Rapid Seismic Risk Assessment of Structures with Gaussian Process Regression

Mohamadreza Sheibani, Ge Ou, and Shandian Zhe

Abstract Risk assessment of structures is an important step to predict damages and losses during natural hazards. The main idea is to fit fragility functions from existing earthquake records. Considerable research has been conducted in this area and various fitting approaches have been suggested. However, existing methods for deriving fragility functions require large training data sets and are designed for a single type of structures each time. This study aims to provide the loss estimation data using supervised learning techniques with a limited amount of observations. Observations are made after the strike of the earthquake based on the responses obtained from randomly selected damaged structures. These observations are used to train the model and prediction of the responses are made for the rest of the structures in the area. A case study is conducted based on the Fukushima 2011 earthquake. It is shown that Gaussian Process Regression (GPR), can provide an integrated model prediction for a group of structures with high accuracy and low uncertainties. This way, not only the predictions are made by a single model for different types of structures, but also the number of observations is very small compared to the existing methods.

Keywords Seismic damage prediction · Risk assessment · Supervised learning · Gaussian Process Regression · Fukushima earthquake

15.1 Introduction

One of the main concerns with damage assessment after an earthquake is about the understanding of the extent of damage and destruction caused by the ground motion shortly after the strike. This information can help authorities recognize the most damaged areas and structures expeditiously, and better manage and dispatch reinforcement and rescue teams. One of the main techniques which is commonly used in risk assessment of structures are the fragility functions [1]. In this approach, a number of ground motion records are collected and scaled and then applied to the structure in order to have a wide range of responses for a structure. Fragility curves are then fitted to the cumulative probability distribution of the responses for a desired Intensity Measure (IM) of the ground motions [2]. This method can reliably predict the damage states of structures in cases where there is a plentiful amount of data available [1]. Some of the notable previous works in this field can be found in [1, 3–5]. However, fragility functions do not perform well in cases where provided data is sparse. Most commonly, if a number of different structures are concerned, a separate fragility curve needs to be calculated for each type of structure. If the data is combined for different types of structures, and one curve is fitted, fragility curves will not be distinctive for different damage states [3]. On the other hand, machine learning methods provide much better results in cases of prediction based on a limited amount of observations. In contrast to fragility functions which only consider one property of the ground motion signal, such as Peak Ground Acceleration (PGA), or Spectral Acceleration (Sa), regression learning methods can be fed as many features as desired. Machine learning methods has been implemented to seek solutions in earthquake science for a long time. One of the most common methods in this area, Artificial Neural Networks (ANN), has been widely used in order to predict the responses of structures using huge training sets [6–9]. However, in the current approach, models are being trained with different earthquake motions and are not specific to one single event.

In the post-hazard situation, one may have to visually inspect the whole area to assess the damage level of different buildings. Such data that reflect the observations of the post-seismic building damage conditions have not been integrated

M. Sheibani (✉) · G. Ou
Department of Civil and Environmental Engineering, University of Utah, Salt Lake City, UT, USA
e-mail: m.sheibani@utah.edu

S. Zhe
School of Computing, University of Utah, Salt Lake City, UT, USA

A. Linderholt et al., *Dynamic Substructures, Volume 4*, Conference Proceedings of the Society for Experimental Mechanics Series,
https://doi.org/10.1007/978-3-030-12184-6_15

with the predictive models, either fragilities curves or ANN trained models. In this paper, we propose to predict the damage of similar structures in the whole area based on a limited number of visually or instrumentally inspected structures. Visual inspections can be made shortly after the hazard and the information will be sent to the data center for further analysis. Moreover, there may be some structures which are pre-equipped with monitoring equipment, such as accelerometers, and this could be another source of information. Combining these two sources, the data center will train a model to predict the responses for other uninspected structures. In this paper, we aim to train our machine learning model from some limited post-hazard observations, and predict the responses for the larger test set. Data from the 2011 Fukushima earthquake is utilized in the form of 592 ground motions recorded at different locations of the country of Japan. The training set is consisted of 100 randomly selected records and the rest is used for verification of the method. Gaussian Process Regression learning method is used to that end. Four different building types are considered in this study, one of which is randomly selected and assigned to each ground motion record. Finally, the predicted responses are compared to the responses obtained by nonlinear time history analysis.

15.2 Gaussian Process Regression

To implement the Machine Learning (ML) to predict the structure responses, GPR algorithm has been used in this paper. GPR works basically like linear regression but for non-parametric functions. In this case, we have a multi-dimensional vector as the independent variable $\mathbf{x}_i$ and observations y_i are made at different intervals of $\mathbf{x}$. Assuming that all dependent variables, i.e. $y_1, y_2, \ldots, y_n$, are different elements of one point sampled from a multivariate Gaussian distribution, one can relate observations to each other using the covariance matrix $\mathbf{K}$ as follows. Considering the exponential kernel, each element of the matrix $\mathbf{K}$ can be expressed as [10],

$$K_{i,j} = k\left(\mathbf{x}_i, \mathbf{x}_j\right) = \sigma_f^2 \exp\left[-\frac{1}{2}\left(\mathbf{x}_i - \mathbf{x}_j\right)^T \mathrm{diag}\left(\mathbf{m}\right)\left(\mathbf{x}_i - \mathbf{x}_j\right)\right] + \sigma_n^2 \delta_{ij} \tag{15.1}$$

where $\boldsymbol{\theta} = \left[\mathbf{m}, \sigma_f^2, \sigma_n^2\right]$ is the vector of the hyperparameters. The maximum allowable covariance is represented by σ_f^2, the variance of the Gaussian distributed noise affecting the observations is denoted by σ_n^2, and δ_{ij} is the Kronecker delta function. Different choices for the matrix $\mathbf{m}$ can be found in [10]. Using the above-mentioned n observations, the prediction of y_* given x_* is achieved by GPR. In order to predict, two more Matrices need to be defined,

$$\mathbf{k}_* = \left[k\left(x_*, x_1\right) k\left(x_*, x_2\right) \ldots k\left(x_*, x_n\right)\right] \tag{15.2}$$

$$\mathbf{k}_{**} = k\left(x_*, x_*\right) \tag{15.3}$$

As mentioned before, the observations are considered as a sample from a multivariate Gaussian distribution. Based on this assumption, and considering the conditional probability, we have,

$$y_* \mid \mathbf{y} \sim N\left(\mathbf{k}_*\mathbf{K}^{-1}\mathbf{y}, \mathbf{k}_{**} - \mathbf{k}_*\mathbf{K}^{-1}\mathbf{k}_*^T\right) \tag{15.4}$$

Therefore, the mean and variance of the predicted instance can be expressed as

$$\mathrm{E}\left(y_*\right) = \mathbf{k}_*\mathbf{K}^{-1}\mathbf{y} \tag{15.5}$$

$$\mathrm{var}\left(y_*\right) = \mathbf{k}_{**} - \mathbf{k}_*\mathbf{K}^{-1}\mathbf{k}_*^T \tag{15.6}$$

It is clear that in order to have predictions with lower variances, the testing instances should be well covered with the training data.

15.3 Case Study Results and Discussion

15.3.1 Model Description

The structure model which has been used in this paper is consisted to be a multi-story steel frame building. A five story shear frame with the same steel columns for all stories was tested experimentally before at [11] and a numerical model was fitted to its components using the Bouc-Wen nonlinear model. Based on the calibrated nonlinear model, four different structures with the same components but a different number of stories such as a 3-story, a 5-story, a 7-story, and a 9 story model, are considered here. The height of stories are about 0.17 m and the weight of each story is 23.2 kg. Newmark Beta has been used for nonlinear time history analysis of the structures and the time step is considered to be 0.001 s for all time history analyses.

Damage state of a structure is best reflected in the maximum experienced drift ratio. Since the drift ratio can be obtained from relative displacement of each story normalized to the story height, damage states can be defined directly on a hysteresis loop of a typical component. In this case, four different damage states are defined, namely none, slight, moderate, and collapse damage. The hysteresis behavior of the nonlinear model subjected to a cyclic pushover test and the abovementioned damage states are shown in Fig. 15.1. The limit state of slight damage Δs, is considered as the yielding point of the component which is about 1.2 cm. The collapse damage state Δc is considered as 5 cm, and the moderate damage state Δm is taken as half of the displacement of the collapse damage. The considered limit states are shown in Fig. 15.1 and described in Table 15.1.

15.3.2 Prediction Objective

Since in real life we get a limited chance to rapidly identify the extent of damage in different areas, the training set size is considered to be a small fraction of the whole data. In this case, out of 592 ground motion records available, 100 randomly selected records (∼17%) are used for training purposes and the rest remain untouched to test the model. We might not have

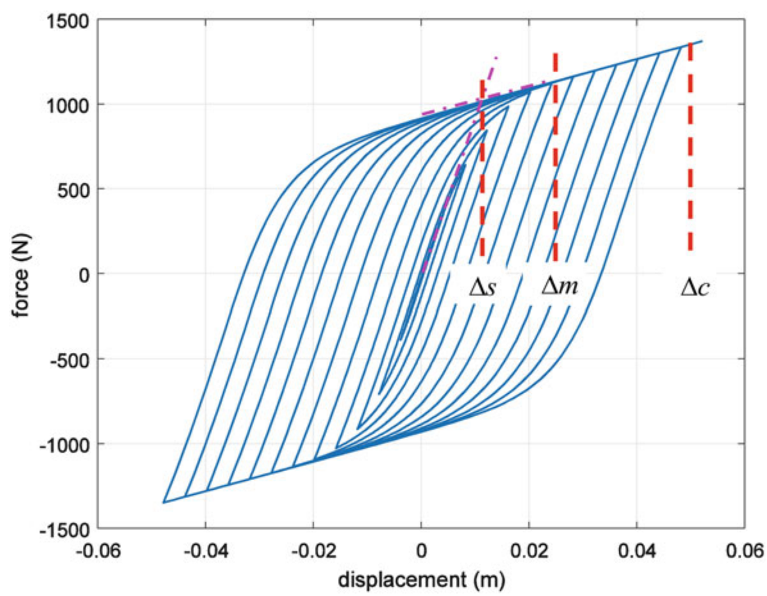

Fig. 15.1 The hysteresis behavior of the component subjected to a cyclic pushover test

Table 15.1 Definition of damage states

Inter-story displacement (m)	Drift ratio	Damage state
ID < 0.012	DR < 0.07	None
0.012 < ID < 0.025	0.07 < DR < 0.15	Slight
0.025 < ID < 0.05	0.15 < DR < 0.29	Moderate
0.05 < ID	0.29 < DR	Collapse

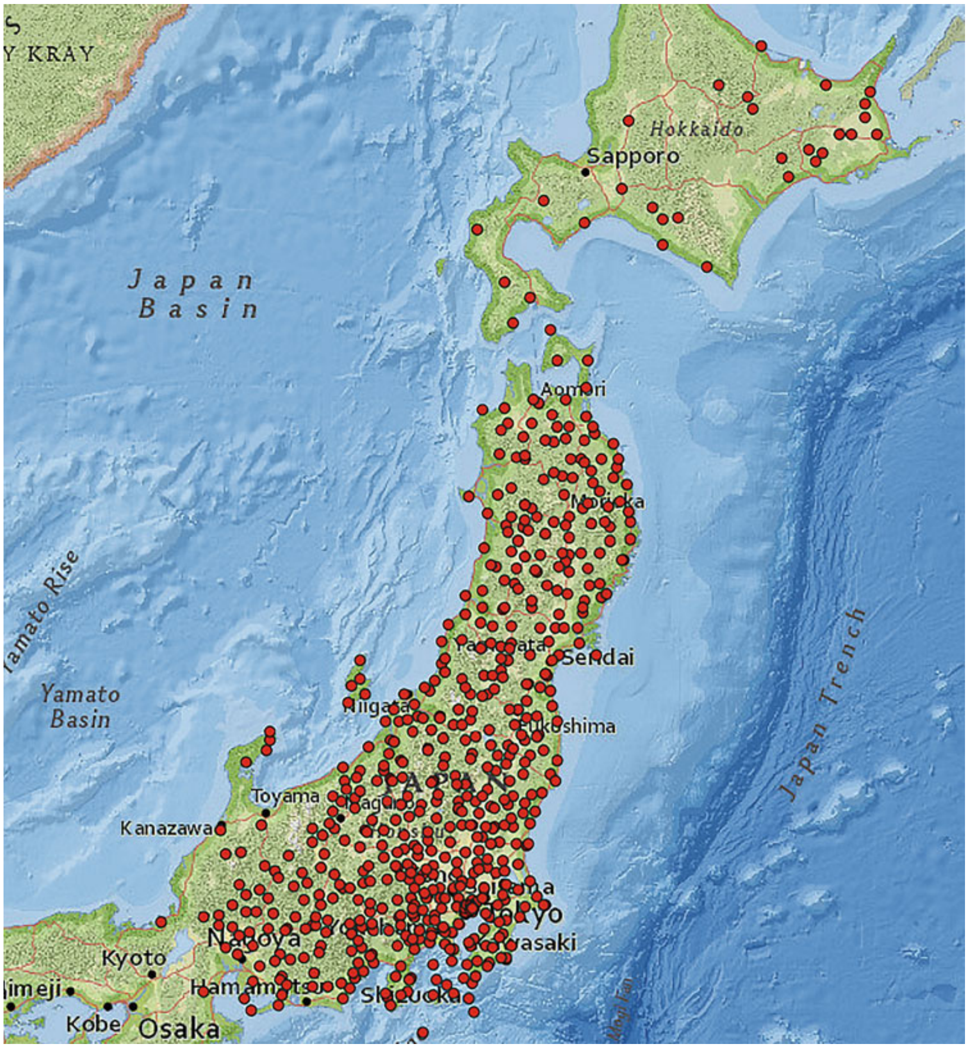

Fig. 15.2 Locations of the recorded ground motions on geographical map of Japan

a chance to record the ground motion at every location that a building is found at in real situations, and thus the attenuation of the ground motion should be considered for other spots. But, in this case, it is assumed that at the location where each ground motion is recorded, one of the four building types is located there and we aim to predict the response of that building. The location of each recorded ground motion with respect to the map of Japan can be seen in Fig. 15.2. The true responses of the structures subjected to the ground motion records are numerically calculated using the nonlinear Newmark Beta method, based on the Bouc-Wen components explained in Sect. 15.3.1. These simulations represent the inspections which are made in real situations.

15.3.3 Results

Supervised machine learning techniques are used in order to help us predict the responses using a trained model. Various supervised regression techniques are available in this field, however, one of the most robust techniques is GPR, which has been used in this paper. One of the main advantageous of GPR is that it provides us with a statistical representation of the prediction, and thus one can see both the mean value and the confidence interval of the predicted value.

In order to train the model, the first stage is defining the features which are going to represent our instances. Two major aspects need consideration in deriving the response of a structure subjected to an earthquake. First, the ground motion signal which carries a significant amount of information with it. Second, the properties of the structure itself, such as the number

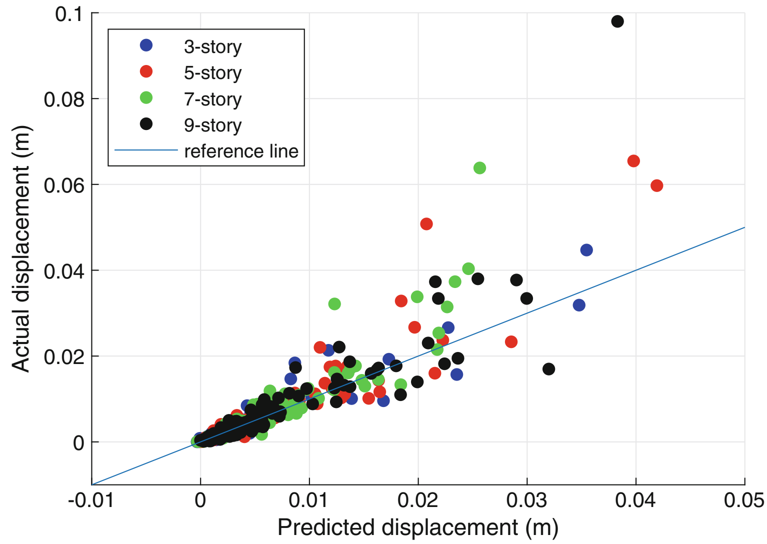

Fig. 15.3 Predicted versus actual maximum displacements for the test set

Table 15.2 Prediction accuracy for each damage state

Damage state	Number of training set	Number of test set	Prediction accuracy %
None	84	423	98.1
Slight	11	48	75.0
Moderate	3	16	31.3
Collapse	2	5	0.0
Total	100	492	92.7

of stories, construction materials, lateral resisting system, etc. Therefore, our model should be trained with a combination of ground motion features and structural features. In this case, nine features are extracted from each ground motion signal, and since the structures are assumed to be identical with only a different number of stories, only one feature is considered for the structures. More information concerning the ground motion features can be found in [12]. Consequently, the model is trained with the above-mentioned features as the feature space and the maximum experienced drift ratio as the label space.

Matlab's GPR modeling command is used in order to train the model. Optimized hyperparameters are obtained and the values of each feature are normalized to unity. The predicted versus actual labels are plotted in Fig. 15.3 for the testing set.

It can be seen in Fig. 15.3 that the trained model has predicted the responses with acceptable accuracy. However, there are some deviations where the components go into the nonlinear phase, and the reason is that the model has been trained with few instances where nonlinear behavior happens. This statement can be illustrated if the output is discretized and the accuracy of each damage state is calculated separately, as in Table 15.2. In order to better clarify this issue, the number of instances in the training set as well as the number of the instances in the test set and their prediction are compared based on their labels in Fig. 15.4a. Moreover, the prediction results are shown on a geographical map of Japan in Fig. 15.4b.

As mentioned earlier, GPR provides a 95% confidence interval for each prediction. Therefore, evaluating the results should not be merely based on the mean values. Confidence intervals as well as the damage limit states are shown in Fig. 15.5 for each prediction. Based on this information, classification of the predicted values is performed from another aspect in Table 15.3. Table 15.2 shows the coverage area of the 95% confidence interval for each damage state. For instance, if the lower bound and upper bound of the confidence interval lies in the same zone as the true response, it is considered to be an exact prediction. On the other hand, if the lower bound is in one zone and the upper bound lies one zone away, and the true response is in either of these zones, it is stated as ±1 level of damage state and so on.

Considering Table 15.3 results, it can be said that the model delivers an accurate result, such that for none damage state, 99.5% of the times the 95% confidence interval includes the true response's zone or, at most, 1 level beside that. This percentage decreases to 93.8% for the slight damage state and to 75% for the moderate damage state. Finally, it can be stated that for the collapse damage state, the 95% confidence interval covers at most two zones beside the true response, 60% of the time. As mentioned earlier, the reduction of accuracy for higher damage states was expected since the GPR model is trained with a limited number of instances at these damage states. Looking at the cumulative results, 75% of the times we are 95%

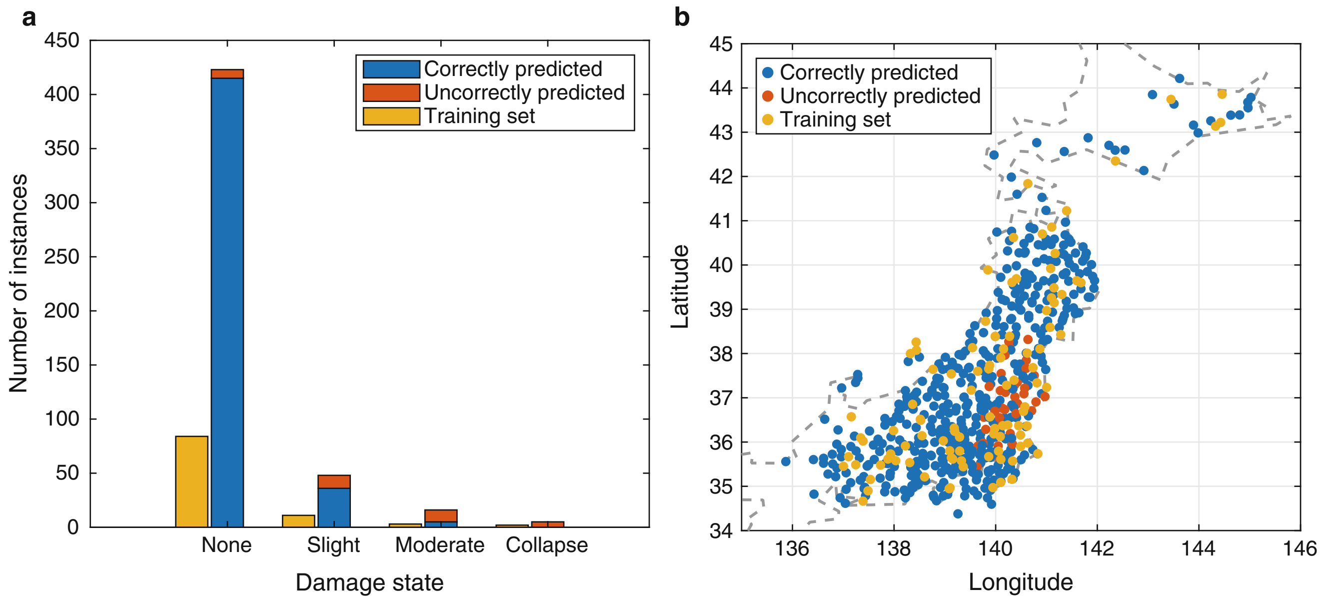

Fig. 15.4 (**a**) Prediction accuracy with respect to number of instances for each damage state, (**b**) correctness of the predicted labels on the geographical map of Japan

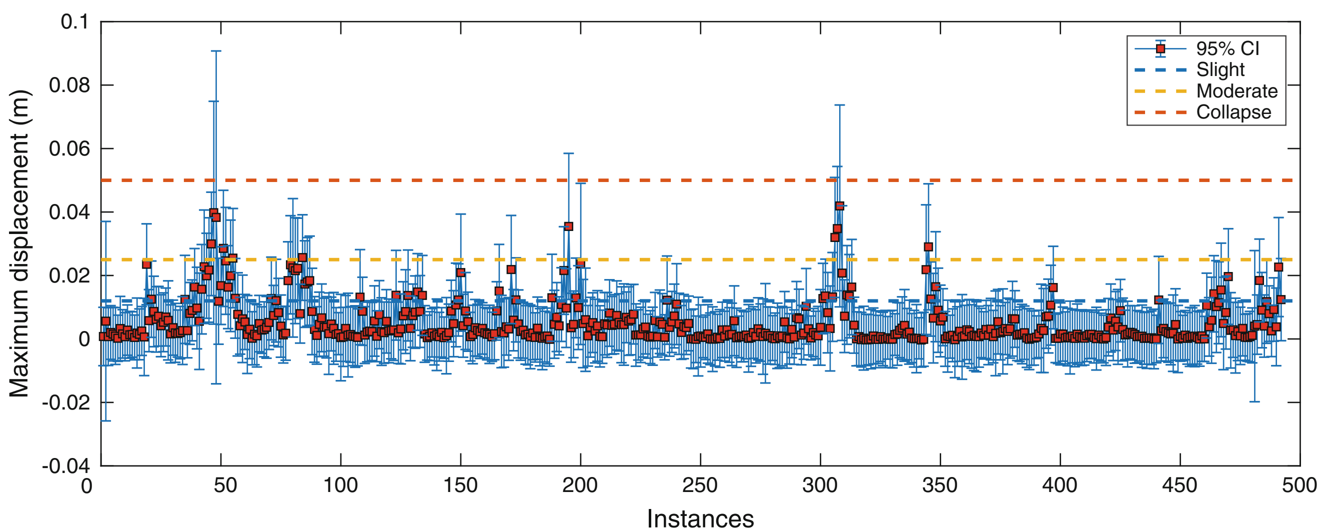

Fig. 15.5 Distribution of the predicted labels along with the 95% confidence intervals

Table 15.3 Predictions based on the 95% confidence interval

Damage state	Total no.	Exact		±1 level		±2 level	
		No.	%	No.	%	No.	%
None	423	369	87.2	52	12.3	2	0.5
Slight	48	1	2.1	44	91.7	0	0.0
Moderate	16	0	0.0	12	75.0	2	12.5
Collapse	5	0	0.0	0	0.0	3	60.0
Cumulative	492	370	75.2	478	97.1	485	98.5

confident that we have the exact prediction of our responses and, for 97.1% of the time, this confidence predicts the exact damage state level or at most one damage state level apart.

15.4 Conclusion

We propose to develop a model which utilizes limited inspection observations after earthquakes to predict building damage conditions based on Gaussian Process Regression. GPR model was able to predict responses with a satisfying accuracy of 92.7%. Moreover, considering the 95% confidence intervals for the predicted data, it was demonstrated that the model is 95% certain to predict the responses within at most one damage state apart, 97.1% of the time. Using this method, predictions can be made within a short period of time after the natural hazard for all the buildings in a vast area.

References

1. Noh, H.Y., Lignos, D.G., Nair, K.K., Kiremidjian, A.S.: Development of fragility functions as a damage classification/prediction method for steel moment-resisting frames using a wavelet-based damage sensitive feature. Earthq. Eng. Struct. Dyn. **41**(4), 681–696 (2012)
2. Kafali, C., Grigoriu, M.: Seismic fragility analysis: application to simple linear and nonlinear systems. Earthq. Eng. Struct. Dyn. **36**(13), 1885–1900 (2007)
3. King, S., Kiremidjian, A., Pachakis, D., Sarabandi, P.: Application of empirical fragility functions from recent earthquakes. In: Proceedings of the 13th World Conference on Earthquake Engineering, Vancouver, BC, Canada. Paper (No. 2829) (2004)
4. Barbat, A.H., Pujades, L.G., Lantada, N.: Performance of buildings under earthquakes in Barcelona, Spain. Comput. Aided Civ. Inf. Eng. **21**(8), 573–593 (2006)
5. Shibata, A.: Estimation of earthquake damage to urban systems. Struct. Control Health Monit. **13**(1), 454–471 (2006)
6. Molas, G.L., Yamazaki, F.: Neural networks for quick earthquake damage estimation. Earthq. Eng. Struct. Dyn. **24**(4), 505–516 (1995)
7. De Lautour, O.R., Omenzetter, P.: Prediction of seismic-induced structural damage using artificial neural networks. Eng. Struct. **31**(2), 600–606 (2009)
8. Morfidis, K., Kostinakis, K.: Approaches to the rapid seismic damage prediction of r/c buildings using artificial neural networks. Eng. Struct. **165**, 120–141 (2018)
9. Lagaros, N.D., Papadrakakis, M.: Neural network based prediction schemes of the non-linear seismic response of 3D buildings. Adv. Eng. Softw. **44**(1), 92–115 (2012)
10. Seeger, M.: Gaussian processes for machine learning. Int. J. Neural Syst. **14**(02), 69–106 (2004)
11. Ou, G.: Robust hybrid simulation with improved fidelity: theory, methodology, and implementation. Doctoral dissertation, Purdue University, West Lafayette (2016)
12. Ye, L., Ma, Q., Miao, Z., Guan, H., Zhuge, Y.: Numerical and comparative study of earthquake intensity indices in seismic analysis. Struct. Design Tall Spec. Build. **22**(4), 362–381 (2013)